

Microvessel surface area, density and dimensions in brain and muscle of the cephalopod *Sepia officinalis*

By N. JOAN ABBOTT† AND M. BUNDGAARD‡

Marine Biological Association Laboratory, Citadel Hill,
Plymouth PL1 2PB, U.K.

(Communicated by P. F. Baker, F.R.S. – Received 28 July 1986)

[Plates 1–6]

The microvasculature of brain and muscle in the cuttlefish *Sepia* was studied with stereological techniques to provide information about the surface area for exchange at the blood–tissue interface which was necessary for a parallel study of the permeability of the blood–brain barrier in *Sepia*. Microvessel density, length, dimensions and volume fraction, and the radius of the ‘Krogh cylinder’ of tissue supplied by each microvessel were also estimated. Vertical lobe (VL) and optic lobe (OL) of brain, outer collar valve muscle (VM) and tentacle muscle (TM) were analysed in 1 µm sections of aldehyde-fixed, Epon-embedded material. ‘Microvessels’ (diameter less than 20 µm) had a surface area density S_V (in the order VL, OL, VM, TM) of 134, 176, 67.9 and 13.8 cm² cm⁻³ respectively. The numbers of microvessels per unit area tissue, Q_A , were 211, 395, 157 and 43 mm⁻² respectively. The length density of microvessels $J_V = 2 \times Q_A$. The microvessel density was significantly greater in synaptic neuropil (NP) than neuron cell body (CB) zones. Total vessel volume density V_V was 3.49, 4.73, 1.88 and 0.28 %, in good agreement with previous estimates using intravascular tracers. Mean microvessel diameter \bar{d} was in the range 4.1–6.5 µm (mode 3.9–4.9 µm). The radius of the Krogh cylinder, R , was 28, 20, 32 and 61 µm. Calculations with the Krogh–Erlang equation show that brain and valve muscle are unlikely to be hypoxic under physiological conditions, while tentacle muscle may be. The vascular parameters correlate well with the known biochemistry of cephalopod tissues. This study represents a detailed analysis of the microvasculature in a complex invertebrate and permits useful comparisons with vertebrate tissues. Values for microvascular S_V , Q_A , J_V and \bar{d} in *Sepia* brain are similar to those of the rat, while *Sepia* muscle vascularity is less than in the rat.

INTRODUCTION

Cephalopod molluscs (including squid, cuttlefish and octopus) are the only non-vertebrate animals to possess a fully closed vascular system in which a substantial blood pressure is generated by the systemic heart. They are thus an

† Permanent address: Department of Physiology, King’s College, Strand, London WC2R 2LS, U.K.

‡ Permanent address: Institute of Medical Physiology A, Panum Institute, University of Copenhagen, Denmark.

ideal group in which to study the comparative physiology of blood-tissue exchange. The anatomy of the gross vasculature in cephalopods has been well described (Isgrove 1909; Williams 1909; Grimpe 1913; Tompsett 1939) and extensive networks of 'capillaries' linking arterial and venous vessels have been illustrated in brain and muscle (Cajal 1924; Young 1971; Bone *et al.* 1981). However, surprisingly little quantitative information is available (Wells 1983). Only Browning (1982) has attempted to quantify tissue vascularity, and because his study of muscle and neural tissue in *Octopus* arms showed a relatively low microvessel density (45 exchange microvessels per square millimetre, corresponding to a maximum diffusion distance of 60–85 µm), he concluded that these tissues would rapidly become hypoxic during activity. This low vascularity has sometimes been taken as representative of all cephalopod tissues (Browning 1982). However, biochemical analysis shows that cephalopod tissues vary greatly in their aerobic-anaerobic capacities (Storey & Storey 1983), so that differences in vascularity would be expected. Further quantitative information on the vascularity of different tissues is therefore needed.

Our own studies of thin sections of tissues from the cuttlefish *Sepia officinalis* suggested a much higher density of microvessels in brain than in muscle. A morphometric analysis was undertaken for two main reasons. Firstly, we have evidence from electron microscopy and radioisotope experiments that *Sepia* has a tight blood-brain barrier, while the blood-muscle interface is relatively leaky (Abbott, Bundgaard & Cserr 1981, 1982, 1985b). However, to compare the permeability of the microvasculature with that of higher vertebrates such as mammals, it is necessary to have a reliable estimate of the surface area (S) for the exchange vessels, so that the permeability coefficient (P) can be calculated from the measured PS (permeability \times surface area) for different molecules. S can be derived by standard morphometric techniques. Secondly, it would be useful to check and to extend the earlier observations concerning tissue vascularity (Young 1971; Bone *et al.* 1981), and the calculations by Browning (1982).

We have accordingly analysed the microvasculature quantitatively in four *Sepia* tissues that we have already studied extensively with physiological techniques: vertical lobe (VL) and optic lobe (OL) of brain, valve muscle (VM) and tentacle muscle (TM) (Abbott, Bundgaard & Cserr 1985a, b). The vertical and optic lobes are representative of the highest levels of coordinated function in cephalopod brain, being responsible for association and learning, and visual analysis respectively (Young 1971), and the two muscles reflect the extremes of vascularization, from valve muscle (highly vascular) to tentacle muscle (poorly vascularized). The valve muscle is the outer collar muscle of the lateral valve flap associated with the funnel (siphon) (Tompsett 1939) and controls water entry into the mantle during ventilation and jetting. The tentacles are kept coiled in pouches under the eyes and are used in prey capture.

In this study we present a morphometric analysis of the microvasculature in the tissues selected, which enables us to calculate the surface area for exchange, and the maximum blood-tissue diffusion distance R (the radius of the Krogh cylinder). It is also possible to give estimates of the vessel diameters, distribution, and

volume density (blood vessel volume fraction). The reliability of the methods used, and the implications of the results, are discussed. A preliminary account of this work has been published (Abbott & Bundgaard 1985).

METHODS

Preparation for microscopy

Sepia of mass 90–750 g were trawled in coastal waters off Plymouth, England, and kept in circulating sea water tanks. One animal (A) was used for thick sections (100–300 µm) and wholermounts. Five others (B 1–5) were used for thin sections (1 µm); of these animals, three had injections of horseradish peroxidase (HRP), and one was perfused with ionic lanthanum (table 1). The electron-dense tracers were included mainly for fine-structural study of vascular permeability (Abbott *et al.* 1981; Bundgaard & Abbott 1987), but acted as a useful check on the completeness of fixative perfusion (see below).

Animals were anaesthetized with 0.2% chloral hydrate in sea water.

TABLE 1. MORPHOMETRIC ANALYSIS

(Details of animals, treatments and tissue sampling (sections).)

animal number	treatment	fixation	animal mass g	number of sections analysed			
				VL	OL	VM	TM
B 1	lanthanum	perfusion	580	5	6	—	—
B 2	no tracer	perfusion	90	4	5	2	—
B 3	HRP 30 min	perfusion	390	5	5	6	2
B 4	HRP 30 min	perfusion	750	5	5	3	2
B 5	HRP 30 min	immersion	90	5	6	—	—

Animal A, thick sections and whole mounts, perfusion fixation

The aorta was exposed and cannulated with fine polythene tubing (outside diameter 1–2 mm), the vena cava was cut to allow perfusate to flow out, and the circulation was flushed with artificial sea water, ASW, containing chloral hydrate anaesthetic (0.1% by mass), perfused at physiological pressure (40–60 cm water) for 3 min to wash out haemocytes. The ASW contained (mm): NaCl 400, KCl 10, CaCl₂ 10, MgCl₂ 52, Tris buffer 5 (pH 7.5). This was followed by perfusion of a solution of Indian ink (Pelikan C 11/1431 a, Günther Wagner) in Formol-saline (10% by volume) for 15 min. Tissues were removed, left in fixative overnight, washed in 0.1 M phosphate buffer (pH 7.4), and either sectioned on an Oxford Vibratome (100–300 µm) or left whole. Tissues and sections were dehydrated in ethanol and cleared in methyl salicylate before photography.

Animals B 1–5, 1 µm sections

In HRP animals (B 3, 4 and 5) the mantle was held open to expose the anterior vena cava, and the tracer (HRP, Sigma Type II, 0.2–0.5 ml ASW containing

250 mg HRP ml⁻¹) was injected into the vein and allowed to circulate for 30 min. The animals were allowed to recover in aerated circulating sea water, and re-anaesthetized towards the end of this period. For animals to be fixed by perfusion (B 1-4), the aorta was cannulated and first perfused with ASW. In the HRP animals (B 3 and 4), and one that had received no tracer (B 2), the perfusion line was then switched to one containing fixative (glutaraldehyde (2.5% by volume) formaldehyde (2% by volume) in 0.1 M cacodylate buffer, pH 7.4, plus 24 g NaCl l⁻¹) and perfusion fixation was continued for 15-20 min. In the lanthanum animal (B 1), ASW perfusion was followed by 10 min perfusion with ASW containing 10 mM LaCl₃, then perfusion with phosphate buffered fixative to precipitate lanthanum ions. In one HRP animal (B 5) tissues were fixed by immersion, and sampling was confined to the superficial regions of the brain.

The cartilage over the brain was sliced away, and brain vertical and optic lobes removed; samples of valve and tentacle muscle were also taken. Tissues were then left in fixative overnight, before being rinsed in buffer and cut into small blocks (0.5-1.0 mm) for further processing. Brain and muscle containing HRP was incubated for 1 h at room temperature in a solution of 3,3'-diamino-benzidine (0.05% by mass) and H₂O₂ (0.01% by volume) in 0.05 M Tris-HCl buffer, pH 7.6 (Graham & Karnovsky 1966), then rinsed in buffer. Subsequent treatment was the same for tissues from all animals. Tissue blocks were post-fixed in OsO₄ in 0.1 M cacodylate buffer, dehydrated in graded ethanol (70, 95, 100% by volume) and embedded in Epon. Sections (1 µm) were cut from randomly selected blocks, half of the sections from tracer-exposed tissue were left unstained, and the others stained with Toluidine Blue. Sections were photographed at standard magnification (234 times) and blood vessel profiles traced onto transparent overlays.

Morphometric analysis

A square grid consisting of a series of uniform short lines (Weibel 1979, p. 378) was placed over the section tracing. The ends of the lines provided a series of points for estimation of volume density, V_V , and the intercepts of the lines with vessel profiles allowed calculation of surface area density, S_V .

We wished to obtain morphometric estimates for total vasculature, and for exchange microvasculature, within each tissue. Most small vessels in *Sepia* are found to have diameters in the range 2-15 µm, so that it is unlikely that significant exchange is contributed by vessels greater than 20 µm diameter. We have accordingly defined 'microvessels' as those with diameters of less than 20 µm.

The following morphometric parameters were measured, separately, for vessels below and above 20 µm diameter (terminology following Weibel (1979)):

- (a) Q_A , number of vessel transections per unit area (mm⁻²);
- (b) J_V , length density, length of vessel per unit volume tissue, = 2 Q_A (mm mm⁻³ or mm⁻²);
- (c) V_V , vessel volume density (mm³ mm⁻³, %), from the percentage of the grid points falling within vessel profiles;
- (d) d , minimum diameter of vessel profiles (µm, tabulated for the first 60 microvessels counted per section);

(e) S_V , surface area density of blood-tissue interface ($\text{cm}^2 \text{cm}^{-3}$ or cm^{-1}), estimated by three separate methods:

(i) $S_V = 2 \sum I_a / \sum L_{\text{total}}$ (Weibel 1979, p. 93) where $\sum I_a$ is the total number of intercepts of the grid lines with the walls of vessels, and $\sum L_{\text{total}}$ is the total length of grid line superimposed on the tracing, corrected for magnification;

(ii) $S_V = 4V_V \sum p_i d_i / \sum p_i d_i^2$ (Haynes 1964), where p_i is the proportion of vessels of diameter class d_i and V_V is the volume density of all vessels considered;

(iii) $S_V = \sum \pi d_i J_{V,i}$, where $J_{V,i}$ is the length density of vessels of diameter class d_i .

Measurements were made on micrographs from two to six sections of the tissues (table 1). The three methods for S_V were applied to the brain of one animal, and the results agreed by a factor of 2 (table 2). The simplest method (e(i)) was used for the rest of the analysis.

Measurements (a), (c) and (e(i)) were made four times for each tracing, by repeated random placements of the grid, and the mean value was taken. The measurements made on each section (replicate) were tabulated for each animal, and an analysis of variance conducted by standard methods to compare variation between replicates with variation between animals (Bailey 1983).

Further parameters were calculated as follows:

(f) $R = 1/\sqrt{\pi} J_V$ (μm), where R is the radius of the Krogh cylinder supplied by each microvessel, and $J_V = 2 Q_A$. Krogh's original papers (1919a, b) used $1/\sqrt{\pi} Q_A$, but this makes no allowances for the tortuosity of the vessels.

(g) \bar{d} , mean microvessel diameter (μm), calculated from the first 60 microvessels on each section (see above, (d)).

Correction for shrinkage

It has been shown that preparation of mammalian and amphibian material for electron microscopy by the present techniques results in shrinkage of the order of 3–5% (Weibel & Knight 1964; Bundgaard & Frøkjaer-Jensen 1982). Checks on ca. 1 mm thick sections of *Sepia* brain during immersion fixation, dehydration and embedding showed that the change in linear dimensions did not exceed 3.5% (brain) and 6% (muscle). Because this was within experimental error, no correction was considered necessary.

RESULTS

Gross morphology of the vascular bed

Figure 1 (plate 1) shows the distribution pattern of the vascular tree in the brain vertical and optic lobes, and in valve and tentacle muscle. In brain, a system of large arteries enters the tissue, and branches in the deep core to finer and finer vessels of the microvasculature, which then drain into venules and veins. The veins run mainly in the medullary core of the optic lobe, but in the vertical lobe there is a system of superficial veins. Openings of the veins to the VL surface are occasionally observed.

Valve muscle has a relatively high vascularity with some evidence of regional

variation, there being a greater concentration of microvessels in the outer and inner zones than in the central zone.

In tentacle muscle there is a major artery running centrally, a major vein with tributaries laterally, and relatively few microvessels in the bulk of the muscle.

The microvasculature

Figure 2*a, c, e, g, i* (plates 2–6) shows photomicrographs of sections used for the present morphometric analysis. In perfuse-fixed material, most vascular spaces are seen as easily recognized clear profiles. In immerse-fixed material, and in a small proportion of vessels in perfuse-fixed tissue which are apparently not filled by fixative, the vessels show up through the presence of dense tracer in the lumen, and through the characteristic appearance of the darkly stained basement membrane and associated perivascular cells (Abbott *et al.* 1981). All recognized vessel profiles were traced on to transparent overlays, as in figure 2*b, d, f, h, j*. In immersion-fixed material some of the HRP-containing microvessels appeared to be relatively collapsed, with star-shaped lumina; vessel dimensions were therefore approximated by a circle or oval passing through the furthest extensions of the profile (figure 3). Justification for this approximation is considered below. The tracings were used for the subsequent morphometric analysis.

Morphometric analysis

(a) Surface area density S_V

The surface area density of the blood–brain (microvessel) interface was estimated by three methods (see above) for animal number B 1 (table 2). The results do not differ by more than a factor of two. The simplest and least biased method (*e(i)*) was therefore used for all subsequent analyses (tables 3–6).

(b) Inter-animal and inter-replicate variation

To detect any differences between animals, which might be caused by the different treatments, the results of morphometric analysis are presented for each animal separately, as well as for all animals pooled, in tables 3–6. Analysis of variance indicates some variation between animals which is greater than that between replicates (p less than 0.05) for certain parameters. The possible reasons for these differences are discussed below.

(c) Mean microvessel diameter, \bar{d} μm

In order to calculate how many microvessels needed to be analysed for a reliable estimate of mean diameter, a running mean was calculated at intervals of ten microvessels, for each of the four tissues. The error of the mean fell to less than

DESCRIPTION OF PLATE 1

FIGURE 1. Gross morphology of the vascular bed in *Sepia* tissues. Cleared thick sections of ink-injected vessels, (a) vertical lobe, (b) optic lobe, (c) valve muscle, (d) tentacle muscle, (e) wholmount, valve muscle. In the preparation used for (a), the superior and inferior frontal lobes were left attached, in order not to disrupt the vessels of the vertical lobe. Blocks used for the morphometric analysis in the rest of the paper were taken from the vertical lobe only. Scale bar 1 mm.

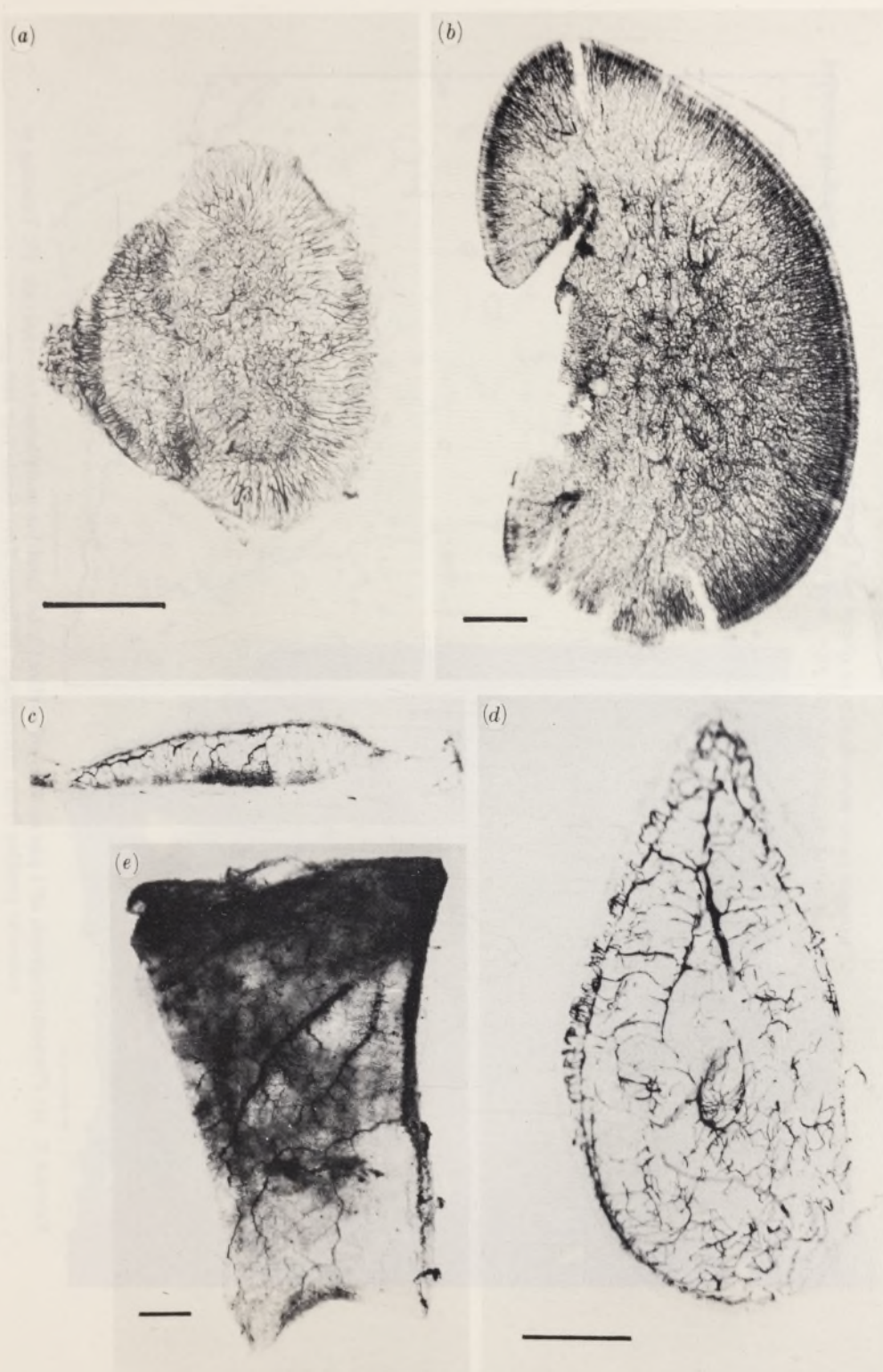


FIGURE 1. For description see opposite.

(Facing p. 464)

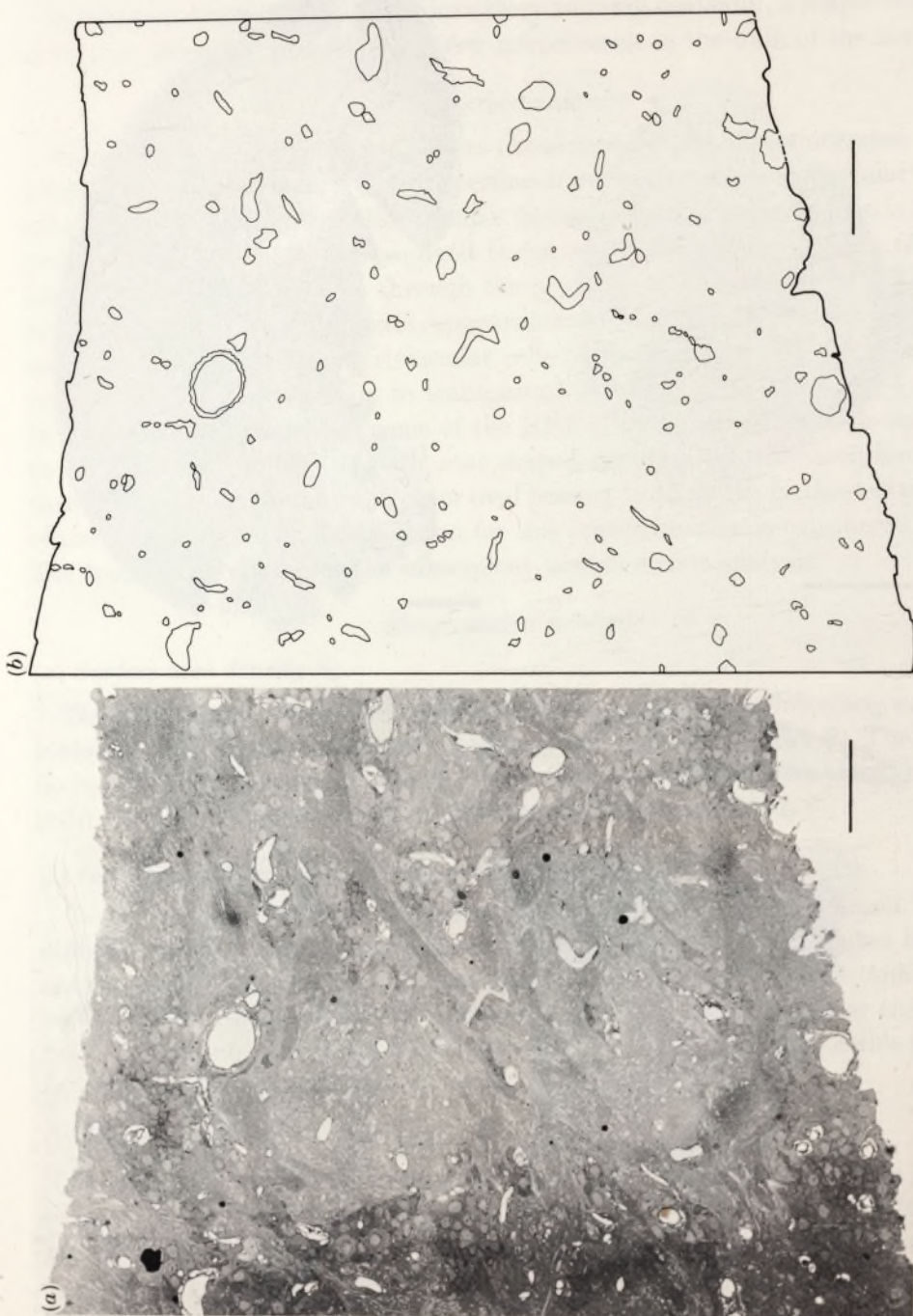


FIGURE 2. (a) Photomicrograph of 1 μm section of vertical lobe used for morphometric analysis. (b) Tracing of vascular profiles from micrograph in figure 2(a). Scale bar 100 μm .

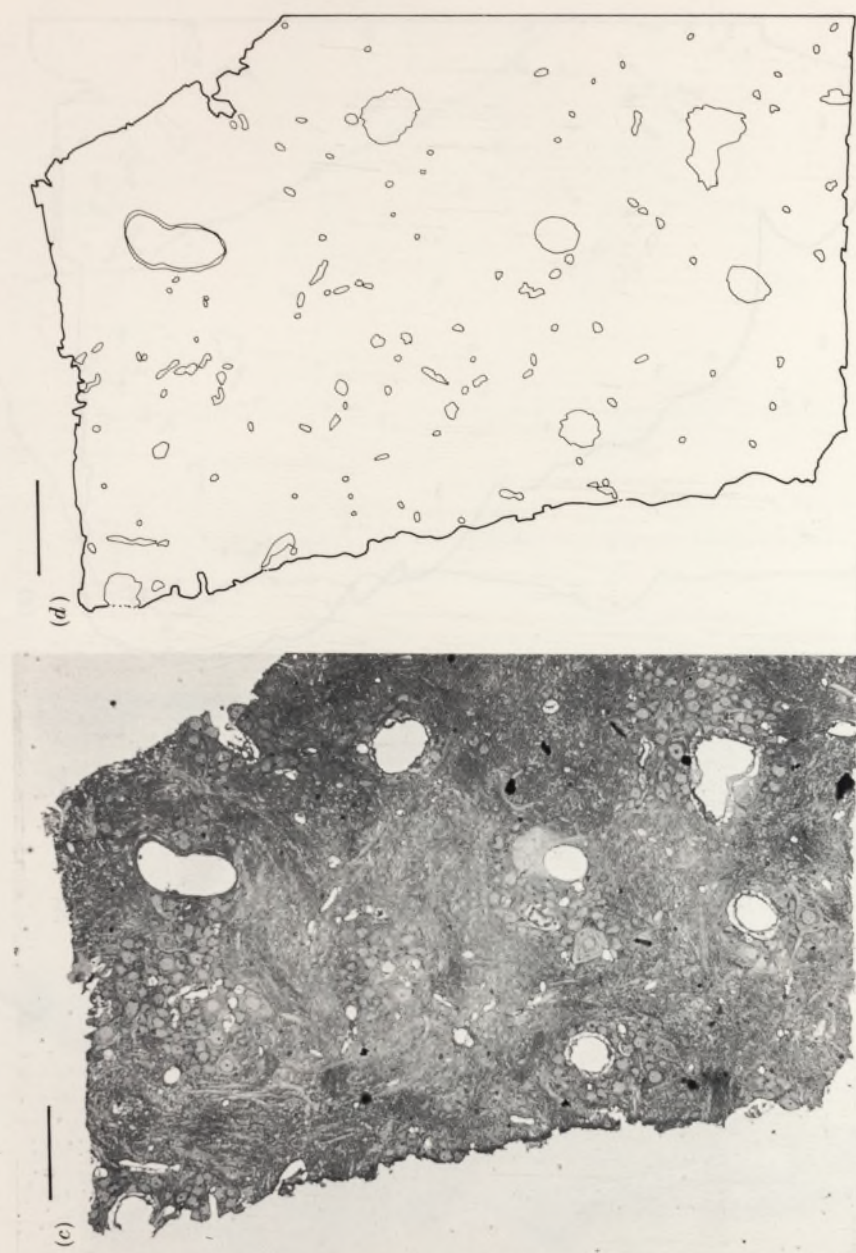


FIGURE 2. (c) Photomicrograph of 1 μm section of optic lobe used for morphometric analysis. (d) Tracing of vascular profiles from micrograph in figure 2(c). Scale bar 100 μm .

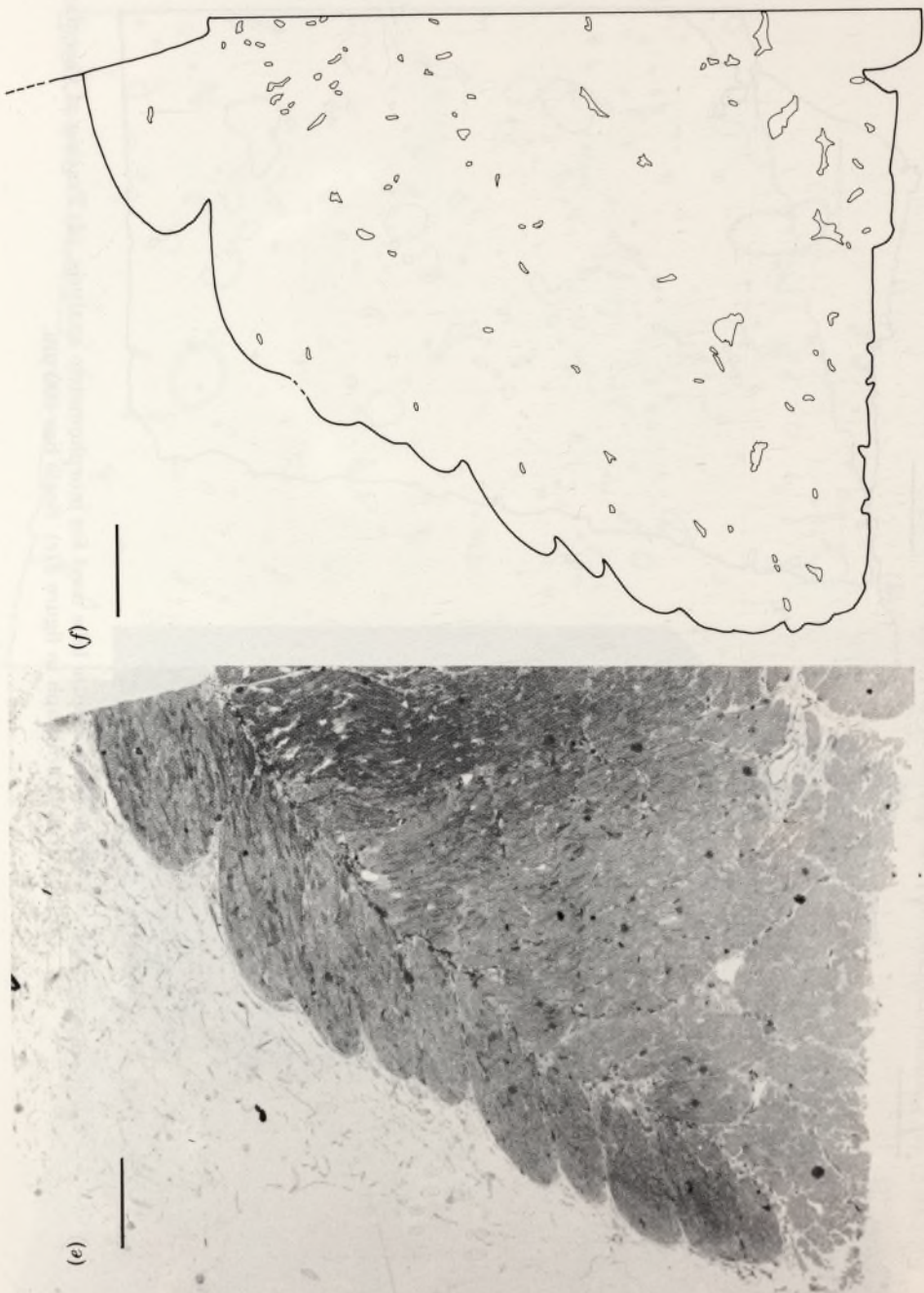


FIGURE 2. (e) Photomicrograph of 1 μm section of valve muscle used for morphometric analysis. (f) Tracing of vascular profiles from micrograph in figure 2(e). Scale bar 100 μm .

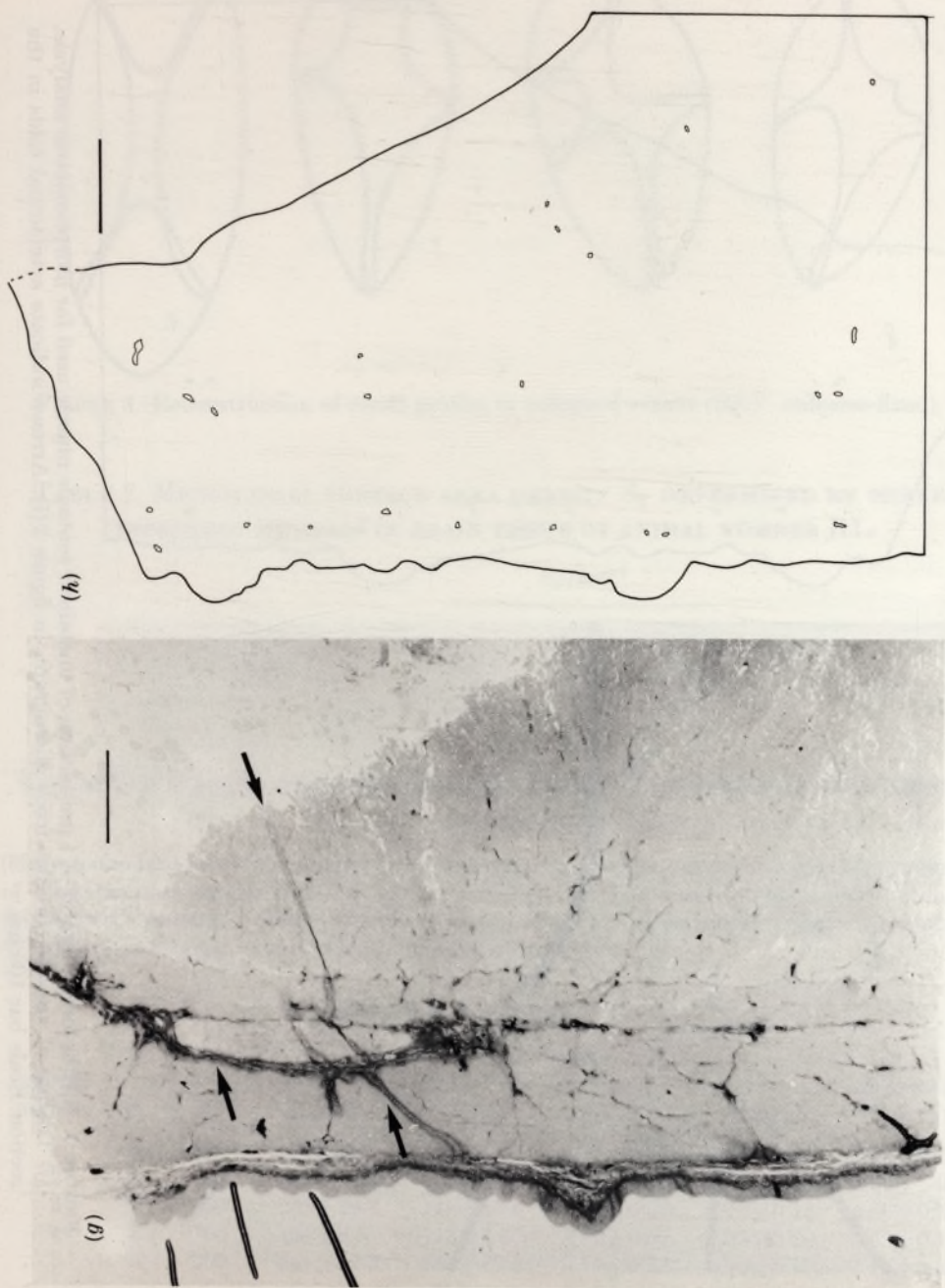


FIGURE 2. (g) Photomicrograph of 1 μm section of stained tentacle muscle used for morphometric analysis.
 (h) Tracing of vascular profiles from micrograph in figure 2 (i), see plate 6. Arrows indicate artefactual folds in the section. Scale bar 100 μm .

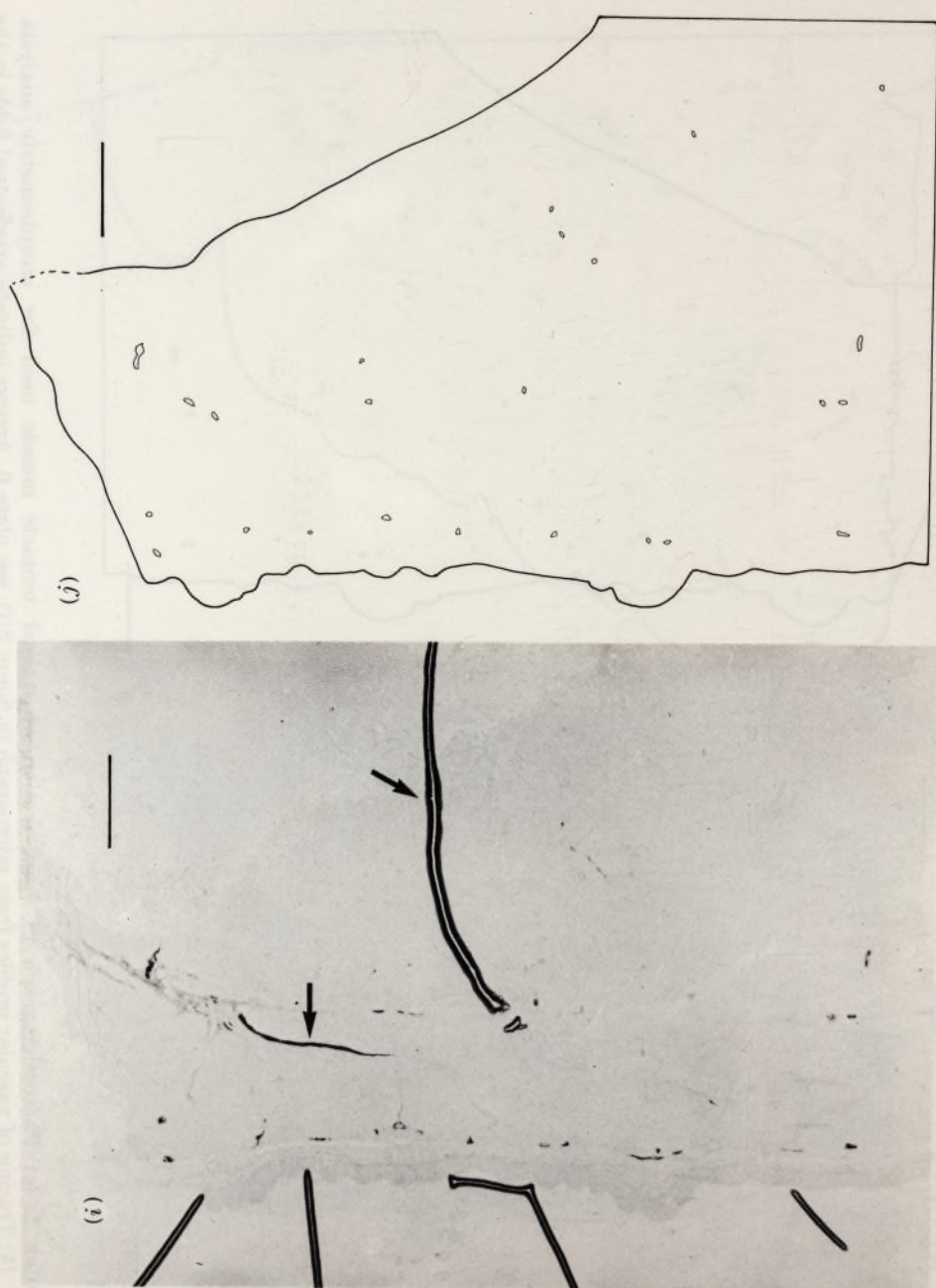


FIGURE 2. (i) Photomicrograph of 1 μm section of unstained tentacle muscle used for morphometric analysis.
(j) Tracing of vascular profiles from micrograph in figure 2 (i). Arrows indicate artefactual folds in the section. Scale bar 100 μm .

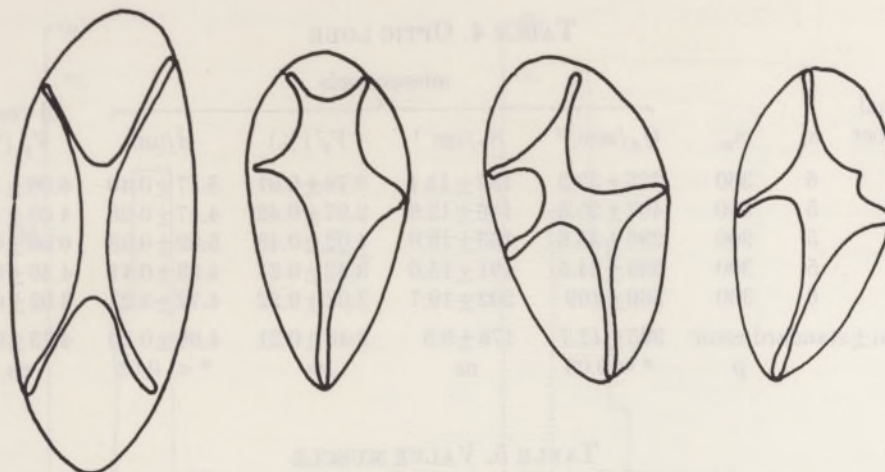


FIGURE 3. Reconstruction of vessel profiles in collapsed vessels (HRP, immerse-fixed).

TABLE 2. MICROVESSEL SURFACE AREA DENSITY S_V DETERMINED BY THREE DIFFERENT METHODS IN BRAIN TISSUE OF ANIMAL NUMBER B1

method	S_V/cm^{-1}		
	(e(i))	(e(ii))	(e(iii))
tissue VL	112.2	112.2	70.8
OL	156.7	217.6	119.5

TABLES 3-6. VESSEL MORPHOMETRIC PARAMETERS MEASURED FOR EACH TISSUE (VL, OL, VM, TM RESPECTIVELY)

(Mean \pm standard error. n_s , number of sections; n_m , number of vessels analysed; Q_A , number of vessel transections per mm^2 ; S_V , surface area density; V_V , vessel volume density; \bar{d} , mean microvessel diameter. † Standard error of mean in final line of each table is based on number of animals; in the rest of the table, on number of sections.)

TABLE 3. VERTICAL LOBE

animal number	n_s	n_m	microvessels				all vessels $V_V/(\%)$
			Q_A/mm^{-2}	S_V/cm^{-1}	$V_V/(\%)$	$\bar{d}/\mu\text{m}$	
1	5	300	172 \pm 11.7	112 \pm 1.9	2.20 \pm 0.88	6.73 \pm 0.17	2.68 \pm 0.40
2	4	240	221 \pm 32.2	150 \pm 33.4	3.35 \pm 0.78	6.03 \pm 0.32	3.64 \pm 1.06
3	5	300	258 \pm 22.3	148 \pm 10.6	2.89 \pm 0.09	6.76 \pm 0.18	4.36 \pm 0.39
4	5	300	164 \pm 8.6	113 \pm 3.6	3.16 \pm 0.07	7.53 \pm 0.20	3.63 \pm 0.15
5	5	300	241 \pm 12.3	148 \pm 15.5	3.10 \pm 0.28	5.56 \pm 0.19	3.14 \pm 0.28
† mean \pm standard error			211 \pm 18.6	134 \pm 8.8	2.94 \pm 0.20	6.52 \pm 0.34	3.49 \pm 0.28
p			* < 0.01	ns	ns	* < 0.01	ns

5% after counting between 70 and 110 vessels. By counting the first 60 microvessels per section, over two to six sections, reliable means were thus obtained in brain and valve muscle. The lower vascular density in tentacle muscle meant that the means for each animal were based on fewer microvessels (50 and 55) so these values are less reliable.

TABLE 4. OPTIC LOBE

animal number	n_s	n_m	microvessels				all vessels V_V (%)
			Q_A/mm^{-2}	S_V/cm^{-1}	V_V (%)	$\bar{d}/\mu\text{m}$	
1	6	360	325 ± 39.3	157 ± 13.1	3.78 ± 0.91	5.47 ± 0.40	6.08 ± 1.25
2	5	300	407 ± 20.6	156 ± 13.9	2.97 ± 0.42	4.47 ± 0.26	4.09 ± 1.19
3	5	300	296 ± 35.6	153 ± 19.0	4.02 ± 0.48	5.82 ± 0.35	6.06 ± 0.69
4	5	300	380 ± 24.5	191 ± 15.0	3.52 ± 0.21	4.33 ± 0.41	4.40 ± 0.43
5	6	360	569 ± 109	202 ± 19.7	3.02 ± 0.22	4.72 ± 0.23	3.02 ± 0.22
† mean \pm standard error			395 ± 47.7	176 ± 9.5	3.46 ± 0.21	4.96 ± 0.29	4.73 ± 0.59
p			* < 0.05	ns	ns	* < 0.05	ns

TABLE 5. VALVE MUSCLE

animal number	n_s	n_m	microvessels				all vessels V_V (%)
			Q_A/mm^{-2}	S_V/cm^{-1}	V_V (%)	$\bar{d}/\mu\text{m}$	
2	2	120	184	67.0	1.66	4.66	1.66
3	6	360	146 ± 12.1	74.5 ± 9.5	2.04 ± 0.15	4.74 ± 0.20	2.04 ± 0.15
4	3	180	143 ± 8.4	62.2 ± 3.8	1.36 ± 0.01	4.94 ± 0.21	1.93 ± 0.27
† mean \pm standard error			157 ± 13.1	67.9 ± 3.6	1.69 ± 0.20	4.78 ± 0.08	1.88 ± 0.11
p			ns	ns	* < 0.05	ns	ns

TABLE 6. TENTACLE MUSCLE

animal number	n_s	n_m	microvessels				all vessels V_V (%)
			Q_A/mm^{-2}	S_V/cm^{-1}	V_V (%)	$\bar{d}/\mu\text{m}$	
3	2	50	31.5	11.1	0.36	4.65	0.36
4	2	55	54.5	16.5	0.20	3.55	0.20
mean			43	13.8	0.28	4.10	0.28
p			* < 0.05	ns	ns	ns	ns

* p less than 0.05 indicates that for this parameter, variation between animals is greater than between replicates (sections).

ns, Not significant.

(d) Microvessel diameter distribution

The distribution of microvessel diameters in each tissue from all animals pooled is shown as histograms in figure 4. The modal diameter, d_m (the diameter corresponding to the peak frequency) can be derived from these graphs and is in the range 3.9–4.9 μm for the different tissues (table 7).

(e) Morphometric parameters

A summary of the measured and calculated parameters is given in table 7 and figure 5. Table 7 also includes values for the rat.

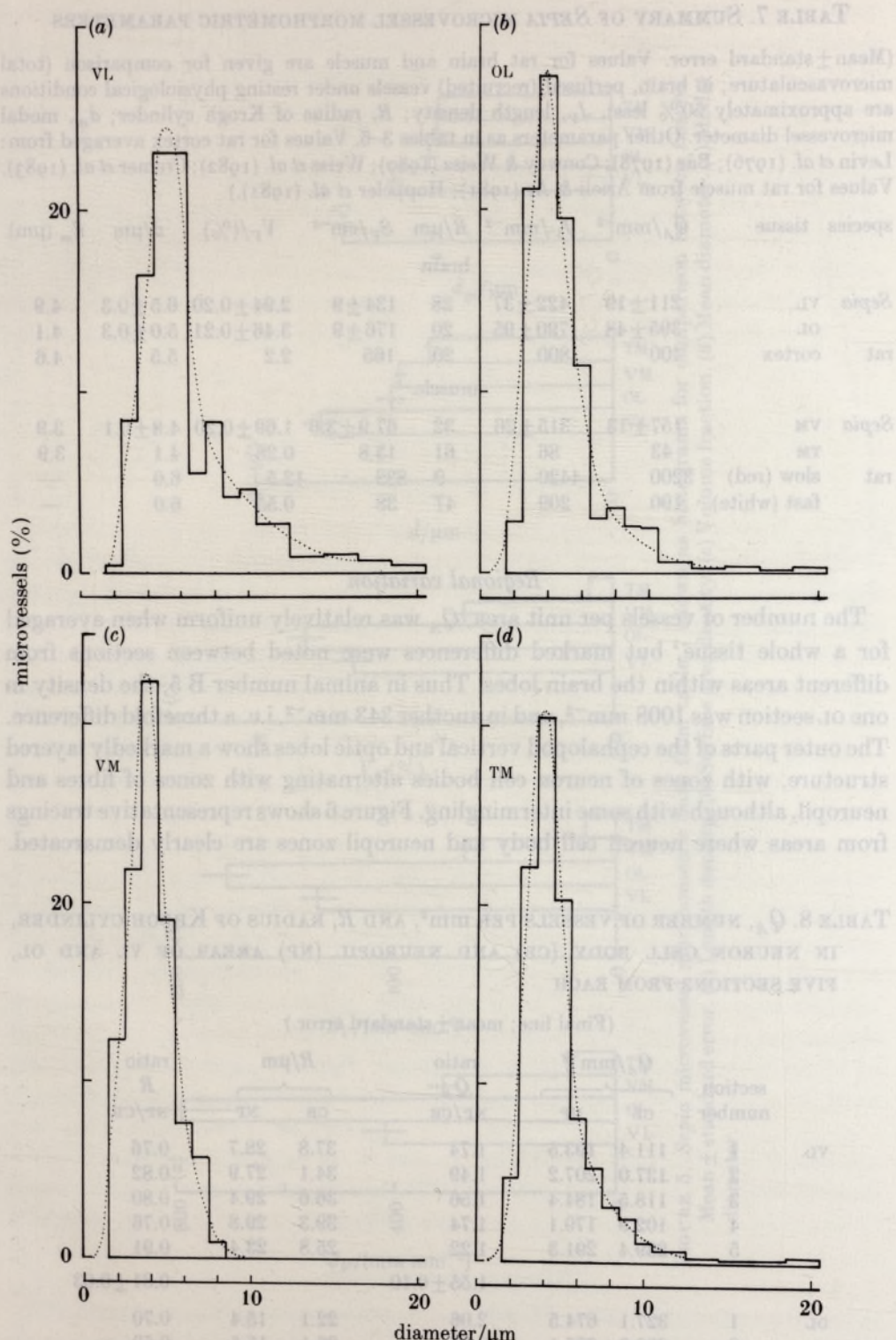


FIGURE 4. Distribution of microvessel diameters, data from all animals pooled. Histograms showing the percentage of microvessels sampled falling into diameter categories 2–20 µm.

TABLE 7. SUMMARY OF *SEPIA* MICROVESSEL MORPHOMETRIC PARAMETERS

(Mean \pm standard error. Values for rat brain and muscle are given for comparison (total microvasculature; in brain, perfused (recruited) vessels under resting physiological conditions are approximately 50% less). J_V , length density; R , radius of Krogh cylinder; d_m , modal microvessel diameter. Other parameters as in tables 3-6. Values for rat cortex averaged from: Levin *et al.* (1976); Bär (1978); Conway & Weiss (1980); Weiss *et al.* (1982); Cremer *et al.* (1983). Values for rat muscle from Arieli & Ar (1981); Hoppeler *et al.* (1981).)

species	tissue	Q_A/mm^{-2}	J_V/mm^{-2}	$R/\mu\text{m}$	S_V/cm^{-1}	$V_V/(\%)$	$\bar{d}/\mu\text{m}$	$d_m(\mu\text{m})$
brain								
<i>Sepia</i>	VL	211 \pm 19	422 \pm 37	28	134 \pm 9	2.94 \pm 0.20	6.5 \pm 0.3	4.9
	OL	395 \pm 48	790 \pm 95	20	176 \pm 9	3.46 \pm 0.21	5.0 \pm 0.3	4.1
rat	cortex	400	800	20	165	2.2	5.5	4.6
	muscle							
<i>Sepia</i>	VM	157 \pm 13	315 \pm 26	32	67.9 \pm 3.6	1.69 \pm 0.20	4.8 \pm 0.1	3.9
	TM	43	86	61	13.8	0.28	4.1	3.9
rat	slow (red)	3200	4420	9	833	12.5	6.0	—
	fast (white)	190	209	41	38	0.55	6.0	—

Regional variation

The number of vessels per unit area, Q_A was relatively uniform when averaged for a whole tissue, but marked differences were noted between sections from different areas within the brain lobes. Thus in animal number B 5, the density in one OL section was 1008 mm^{-2} , and in another 343 mm^{-2} , i.e. a threefold difference. The outer parts of the cephalopod vertical and optic lobes show a markedly layered structure, with zones of neuron cell bodies alternating with zones of fibres and neuropil, although with some intermingling. Figure 6 shows representative tracings from areas where neuron cell body and neuropil zones are clearly demarcated.

TABLE 8. Q_A , NUMBER OF VESSELS PER mm^2 , AND R , RADIUS OF KROGH CYLINDER, IN NEURON CELL BODY (CB) AND NEUROPILO (NP) AREAS OF VL AND OL, FIVE SECTIONS FROM EACH

(Final line; mean \pm standard error.)

section number	Q_A/mm^{-2}		ratio Q_A NP/CB	$R/\mu\text{m}$		ratio R NP/CB	
	CB	NP		CB	NP		
VL	1	111.4	193.5	1.74	37.8	28.7	0.76
	2	137.0	207.2	1.49	34.1	27.9	0.82
	3	118.5	184.4	1.56	36.6	29.4	0.80
	4	102.9	179.1	1.74	39.3	29.8	0.76
	5	239.4	291.3	1.22	25.8	23.4	0.91
				1.55 \pm 0.10			0.81 \pm 0.03
OL	1	327.1	674.5	2.06	22.1	15.4	0.70
	2	232.9	665.1	2.86	26.1	15.5	0.59
	3	525.3	848.9	1.62	17.4	13.7	0.79
	4	346.6	675.2	1.95	21.4	15.4	0.72
	5	280.8	465.8	1.66	23.8	18.5	0.78
				2.03 \pm 0.22			0.72 \pm 0.04

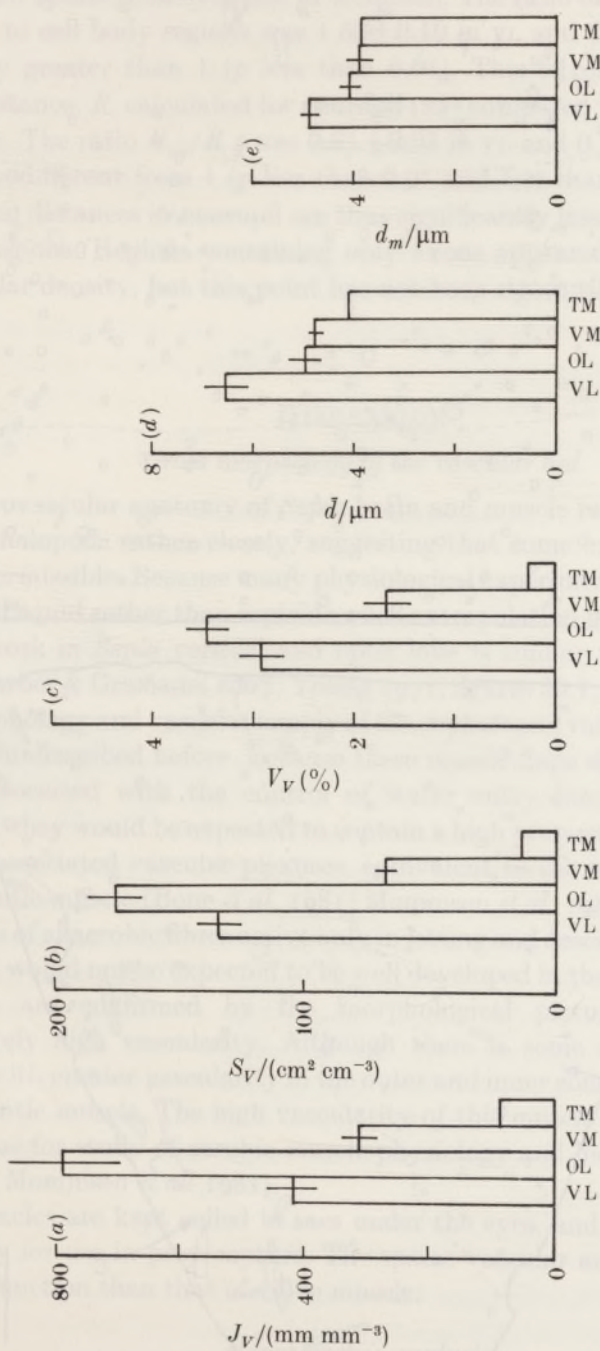


FIGURE 5. *Sepia* microvessel morphometric data from table 7 shown as histograms for comparison between tissues. Mean \pm standard error. (a) Length density. (b) Surface area density. (c) Volume fraction. (d) Mean diameter. (e) Modal diameter.

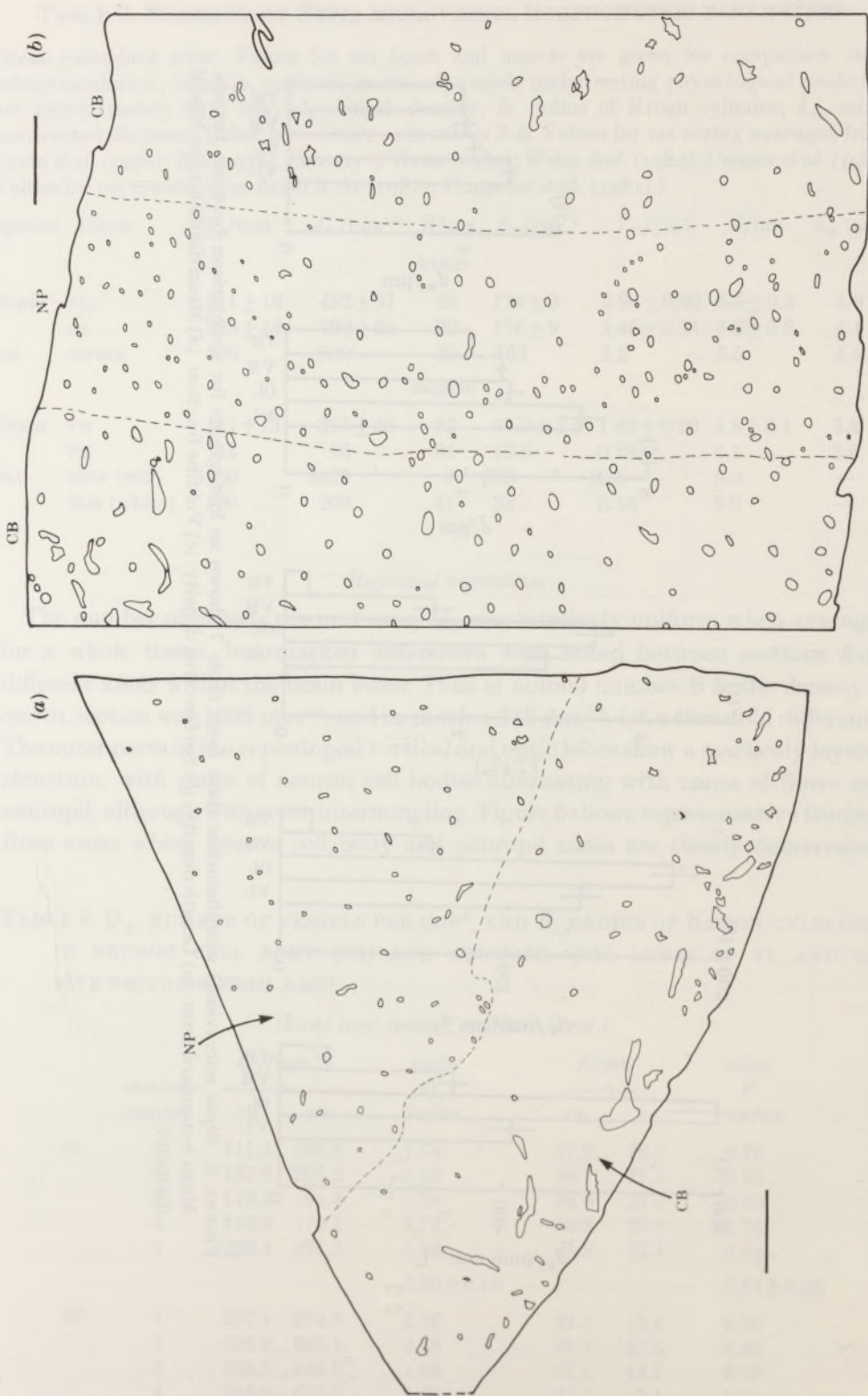


FIGURE 6. Vessel tracings from sections where neuron cell body (CB) and neuropil (NP) regions are clearly demarcated. (a) Vertical lobe, cell bodies of amacrine cell layer. (b) Optic lobe, cell bodies of inner and outer granule cell layer. Scale bar 100 μm .

Table 8 gives vessel counts per unit area over the two zones in a series of sections. The vessel density is clearly higher in regions of fine (synaptic) neuropil than in regions of cell bodies (non-synaptic in molluscs). The ratio of microvessel densities in neuropil to cell body regions was 1.55 ± 0.10 in VL and 2.03 ± 0.22 in OL, both significantly greater than 1 (p less than 0.01). This is reflected in the shorter diffusion distance, R , calculated for neuropil (NP) compared with neuron cell body (CB) regions. The ratio R_{NP}/R_{CB} was 0.81 ± 0.03 in VL and 0.77 ± 0.04 in OL, again significantly different from 1 (p less than 0.01 and less than 0.002 respectively). The diffusion distances in neuropil are thus significantly less than those in neuron cell body regions. Regions containing only axons appeared to have even lower microvascular density, but this point has not been rigorously quantified.

DISCUSSION

Gross morphology of the vascular bed

The microvascular anatomy of *Sepia* brain and muscle resembles that of other coleoid cephalopods rather closely, suggesting that some extrapolation between species is permissible. Because many physiological experiments have been done on octopus and squid rather than sepioids, such extrapolation is often necessary. The vessel network in *Sepia* vertical and optic lobe is similar to that described for *Octopus* (Barber & Graziadei 1967; Young 1971, figures 20.1, 20.2, 20.3 and 20.17).

The morphology and vascular supply of the cephalopod valve muscle appear not to have been described before. Because these muscle flaps show steady rhythmic activity associated with the control of water entry into the mantle during ventilation, they would be expected to contain a high proportion of aerobic muscle fibres and associated vascular plexuses, equivalent to the outer and inner zones of bulk mantle muscle (Bone *et al.* 1981; Mommsen *et al.* 1981). The less vascular central zone of anaerobic fibres active only in jetting and described in mantle (Bone *et al.* 1981), would not be expected to be well developed in the valve muscle. These predictions are confirmed by the morphological picture, which shows a comparatively high vascularity. Although there is some evidence of regional variation, with greater vascularity in the outer and inner zones, this is less marked than in mantle muscle. The high vascularity of this muscle suggests it would be a good tissue for study of aerobic muscle physiology and biochemistry (cf. Bone *et al.* 1981; Mommsen *et al.* 1981).

The tentacles are kept coiled in sacs under the eyes, and are only flicked out occasionally for use in prey capture. The sparse vascular array suggests a more anaerobic function than that of valve muscle.

Morphometric analysis

The prime aim of this study was to produce reliable estimates for the surface area for exchange of the microvasculature in *Sepia* brain and muscle, and to calculate likely maximum diffusion distances between the microvessels and tissue. We have also produced information about the size distribution of microvessels, and about the volume fraction of the tissue occupied by vessels. In the discussion that follows,

the *Sepia* results are compared with the previous cephalopod data, and with equivalent morphometric analyses on a representative small vertebrate, the rat. It would also have been instructive to make the comparison with a cold-blooded vertebrate such as a fish or amphibian, particularly in view of the many physiological parallels between cephalopods and fish (Packard 1972). However, insufficient information is available for the microvasculature of the brain in these groups, and the microvascular data for fish muscle is usually presented with reference to muscle fibre area, rather than section area as here, making comparison difficult.

Reliability of results

This study aimed to estimate microvascular parameters under conditions as close to those of the physiological experiments (Abbott *et al.* 1985b) as possible. The accuracy of the results is now considered.

(a) Shrinkage

This can be assumed to be negligible (see methods).

(b) Alterations produced by fixation

Perfusion fixation was performed with pressures within the physiological range, 40–60 cm water, compared with resting aortic systolic pressures recorded in cephalopods of 20–60 cm water (*Octopus*, Wells (1979)) and 50–100 cm water (squid, Bourne (1982)); no values are available for *Sepia*. The use of continuous perfusion at pressures approaching the peak systolic pressure, rather than pulsatile perfusion as *in vivo*, might have caused some vasodilatation. However, the mean diameter of microvessels in the immerse-fixed optic lobe was within the range of the perfusion-fixed material. In vertical lobe, the mean diameter was greater after perfusion fixation, but because immersion fixation limits sampling to the first 0.5 mm from the tissue surface, a region of the vertical lobe containing predominantly small vessels, this variation can probably be wholly accounted for by the differences in sampling. The method of measurement in collapsed vessels (figure 3) probably introduced some error, but the uniformity of the results suggests the error was small. It is concluded that the preparative procedures do not cause significant distortion of the vessel dimensions. A similar conclusion was reached by Michel *et al.* (1984) from comparison of immerse-fixed with perfuse-fixed frog sciatic nerve microvessels.

(c) Recognition of all recruited vessels

Perfuse fixation shows perfused vessels as open profiles, but occasional microvessels may be patent *in vivo*, yet not filled by fixative because of blockages occurring during fixation. The presence of HRP in the vessels patent *in vivo* means that such vessels show up clearly as grey-black transections on the micrographs, with discernible wall-perivascular structures; these vessels are therefore readily included in the count. In practice, these extra vessels account for only a few percent of the total; this is confirmed by the finding that the microvessel densities in the animal without tracer (B 2) fall within the range of those with tracer. It can

therefore be concluded that the bulk of microvessels perfused *in vivo* show up and are counted in our procedures.

Our micrographs include some vascular profiles that appear as a narrow slit, width *ca.* 2 µm. Because this is close to the resolution of the light microscope, and also approaches the thickness of the sections (nominally 1 µm), it is likely that diameters of less than 3 µm are not recorded with great accuracy. In vertebrates with circulating erythrocytes, the dimensions of the microvessels are largely determined by the dimensions of the corpuscles, so that diameters less than 3 µm are rare. It might be argued that in cephalopods where the blood pigment circulates as polymers of *ca.* 3.7 MDa molecular mass, 35 × 19 nm diameter (Ghiretti-Magaldi *et al.* 1977), there is no such limitation on microvascular size, and vessels of even 1 µm diameter might be found. These would be below the resolution of our methods, and therefore not counted. However, in an extensive survey of thin sections from the present material, at the electron microscope level, vessels of diameter less than 2 µm were rare (Bundgaard & Abbott 1987). Thus ignoring these vessels introduces little error.

A final test of the reliability of our figures comes from a comparison of the vascular volume calculated from our total vascular volume density V_V (total), with that measured by using large intravascular tracers in physiological experiments (Blue dextran, ^{125}I -labelled serum albumin; Abbott *et al.* (1985a)), table 9. The values agree to within 20% in three out of four tissues.

TABLE 9. COMPARISON OF THE TOTAL TISSUE VASCULAR SPACE CALCULATED FROM THE MORPHOMETRIC DATA, WITH PREVIOUS ESTIMATES USING VASCULAR TRACERS (ABBOTT *ET AL.* 1985*a*)

tissue	morphometric study		tracer study: vascular space (ml g ⁻¹) (%) (n)	ratio, vascular space, morphometric: tracer
	total V_V	vascular space, calculated†		
	(mm ³ mm ⁻³) (%)	(ml g ⁻¹) (%)		
VL	3.49 ± 0.28	3.29 ± 0.26	3.43 ± 0.19 (29)	0.96
OL	4.73 ± 0.59	4.46 ± 0.56	5.62 ± 0.21 (23)	0.79
VM	1.88 ± 0.11	1.77 ± 0.10	2.18 ± 0.27 (7)	0.81
TM	0.28	0.26	0.38 ± 0.26 (24)	0.70

† Vascular space was calculated from $V_V/1.06$ to correct for tissue density.

Effect of anaesthesia

Anaesthetized animals were used for both physiological and morphometric studies of the vasculature. The effect of the anaesthetic on the vascular parameters is unknown, but some vasodilatation may be expected. However, the level of anaesthesia was such that valve and tentacle muscle preserved near-normal tone, and the venous sinuses of the head were not engorged with blood, so the results are probably close to those of the normally awake animal. The values for the rat (table 7) are also from anaesthetized animals.

Possibility of recruitment

Our results give no information about whether significant recruitment can or does occur in *Sepia* brain and muscle, although such recruitment has been suggested for the equivalent mammalian tissues (Weiss *et al.* 1982; Renkin 1968). Recent ^{125}I -labelled serum albumin studies suggest that *Sepia* brain O₂ blood volume under good physiological conditions may be slightly less than in conditions of hypoxia (65 %), although this effect was less marked in VL (81 %) and not demonstrable in tentacle muscle (valve muscle not studied) (Abbott 1987). These observations are consistent with recruitment in brain of the same order as suggested for the rat (i.e. ca. 50 % of total brain microvasculature recruited under normal physiological conditions). We have allowed for this possibility in discussions of tissue O₂ tension (table 10). For calculations involving the surface area density, S_V , recruitment will not alter the figures by more than a factor of 2; because estimates for PS of small solutes in rat brain themselves differ by up to a factor of 10 in different studies, we have not thought it necessary to consider the effects of recruitment in detail.

Morphometric parameters

(a) Definition of microvessels

It can be seen from figure 4 that most of the small vessels fall within the range 2–15 µm diameter, with a few in the range 15–20 µm. Thicker-walled vessels (arteries) tended to have diameters in the range 30–120 µm, so that by setting the cut-off point at 20 µm we are reasonably certain to include the bulk of exchange vessels and exclude non-exchange vessels.

(b) Number of microvessel transections per unit area, Q_A

The results presented in tables 3–7 show the high vascularity of *Sepia* brain and valve muscle, and the much lower vascular density of tentacle muscle. The values for brain resemble those in the rat (table 7). There is some regional variation of vascular density within the nervous system, with the highest densities to be found in regions rich in synapses (figure 6 and table 8). This is in good correspondence with results from vertebrate nervous tissue showing that cell bodies with synapses (cerebral cortex, cervical sympathetic ganglion) had a higher vascularity than those without (trigeminal ganglion) (Dunning & Wolff 1937). However, the *Sepia* results are more clearcut, because in cephalopods cell bodies and synapses are spatially separated.

(c) Microvessel length density, J_V

In calculating parameters affected by the contact surface between vessel and tissue, early workers followed Krogh (1919a) in using the number of vessels per unit section area, N_A or Q_A (mm^{-2}). The length of vessel per unit volume, J_V would then be numerically equal to Q_A . However, this assumes that the vessels are straight cylinders cut in perfect cross section, and ignores the effect of tortuosity. When tortuosity is taken into account, and assuming a randomly orientated (isotropic) vessel network, $J_V = 2Q_A$ (Weibel 1979). In cephalopod brain, since the

finest microvessels form an elaborate three-dimensional meshwork without clear parallel arrays, isotropy is a reasonable assumption; furthermore, because the sections are taken in random orientation, this should cancel out any effect of marked vessel orientation. Muscle vasculature tends to be more anisotropic, because vessels generally run aligned to muscle fibres. However, whole mounts of cephalopod valve and mantle muscle show a less ordered array than in vertebrates (figure 1, and Bone *et al.* (1981)), so until further information is available, it is reasonable to assume that the *Sepia* muscle vasculature is also relatively isotropic.

(d) *Vessel volume density, V_V*

The volume density of the total vasculature in the sections (including large vessels) agrees well with the distribution space of vascular tracers in physiological experiments (table 9) in vertical and optic lobe and in valve muscle, less well in tentacle muscle. In all tissues it is likely that the contribution of large vessels was somewhat underestimated in the sectioned material because of their scarcity and the relatively small size of the samples; this is particularly true of the tentacle muscle. As large vessels contribute a proportionately much greater volume than microvessels, this could readily explain the differences observed.

(e) *Microvessel diameters, d, \bar{d}, d_m*

The distribution of microvessel sizes in the different tissues is rather consistent (figure 4), but the mean diameter \bar{d} in vertical lobe is significantly greater than in the other tissues, mainly because of the greater proportion of larger vessels (figure 5). The mean diameters calculated are rather similar to those of rat brain and muscle (table 7). It should be noted, however, that because the calculated mean depends on the size range chosen for the analysis, as well as the frequency distribution within this range, and previous studies have used different 'cut-off' points for microvessels included (e.g. 8 µm, Levin *et al.* (1976); 7.5 µm, Bär (1978); 12 µm, Weiss *et al.* (1982)), a simple comparison of means between different studies can be misleading.

The microvessel modal diameter, d_m , is more consistent (table 7, figure 5) at 4–5 µm, and remarkably close to that of the rat (4.6 µm, Weiss *et al.* (1982)). The similarity between cephalopod and vertebrate microvessels is perhaps surprising because cephalopod microvessel dimensions are not constrained by the size of erythrocytes. It is possible that relatively large vessels are required in cephalopods to keep the total peripheral resistance low, so that the relatively low arterial systolic pressures (mean 30–54 mmHg in different species, Bourne (1982)) can produce adequate tissue blood flow.

(f) *Exchange surface area density, S_V*

The surface area for exchange between blood and tissues was the primary interest of this study. Three methods for S_V are commonly used in stereological studies, and were tested on vertical and optic lobe of animal number B 1 (table 2). Method (e(ii)) (Haynes 1964), $S_V = 4V_V \sum p_i d_i / \sum p_i d_i^2$ is suitable for microvessels of a narrow size range, but the presence of a d^2 term in the equation means that large vessels have a disproportionately large effect on the result; moreover, it relies on accurate knowledge of the volume density of the microvessel population, V_V .

Method (e(iii)), $S_V = \sum \pi d_i J_{V,i}$, relies on a knowledge of $J_{V,i}$ calculated from $Q_{A,i}$ assuming random orientation of microvessels, and accurate measurements of vessel diameters. Method (e(i)), $S_V = 2 \sum I_a / \sum L_{\text{total}}$ uses direct counting of test line intercepts on the section tracings, and does not rely on other measurements or assumptions; it is therefore the preferred method, used for the rest of the analysis. The good agreement between the values derived by the three methods (table 2) demonstrates the internal consistency of the results.

It should be noted that although S_V has generally been determined on light microscopical material, tortuosity of the vascular profiles beyond the resolution of the light microscope is ignored, so that the true S_V tends to be underestimated. The S_V measured at 10000 times magnification (EM) may be as much as 38% greater than at 250 times magnification (LM) (see Weibel (1979), figure 4.27). However, because our aim is to calculate P from PS , for comparison with vertebrates, we have deliberately used methods comparable to previous studies. Moreover, by using predominantly perfuse-fixed material, the effects of tortuosity of collapsed vessel profiles are minimized.

Inter-animal variation

For certain morphometric parameters, notably the microvessel density Q_A , and mean diameter \bar{d} , the variation between animals is greater than that between replicates (sections) taken from the same animal (p less than 0.05 in tables 3–6). Some of the variation no doubt reflects the fact that in the immerse-fixed animal (B 5), sections were taken only from the outer 0.5 mm of vertical and optic lobe, where cell body and neuropil rather than axon tracts predominate, and most vessels are small. Other sources of variation may be the size and weight of the animals (table 1) and inhomogeneities in the vascular bed, e.g. rises in capillary density as p_{O_2} falls during passage through a tissue. However, for the parameter of most interest, S_V , the variation between animals is not significantly greater than that between replicates. Because previous studies have made no attempt to control for inter-animal variation, the results from the present animals are regarded as adequately homogeneous.

Calculation of blood-tissue oxygen gradient

According to the Krogh-Erlang equation (Krogh 1919a),

$$T_0 - T_R = \frac{p}{k} \left[1.15 R^2 \log_{10} \left(\frac{R}{r} \right) - \left(\frac{R^2 - r^2}{4} \right) \right],$$

where T_0 is the oxygen tension in microvessels (atm), T_R the oxygen tension in tissues mid-way between microvessels (atm), R the radius (cm) of cylinder of tissue supplied by each microvessel, r the radius (cm) of microvessels, p the gas exchange, O_2 absorbed $\text{ml g}^{-1} \text{min}^{-1}\dagger$, and k the rate of diffusion of O_2 through 1 cm^2 , and a distance of 1 cm of tissue.

† In the absence of detailed information about tissue O_2 uptake, it is initially assumed that this is equivalent to uptake by the whole animal. However, since brain O_2 uptake in rat may be up to ca. 8.5 times whole body uptake (calculated from a glucose utilization (cortex) of ca. $1 \mu\text{mol g}^{-1} \text{min}^{-1}$ (Cremer *et al.* 1983), calculations for *Sepia* brain O_2 uptake are repeated with an 8.5 times higher O_2 consumption.

If $T_0 - T_R$ is less than T_V , the venous oxygen tension, then the tissue oxygen tension must be positive everywhere within the tissue, while if $T_0 - T_R$ is greater than T_V then some portions of the tissue must suffer from O_2 lack (Krogh 1919a). Browning (1982) calculated $T_0 - T_R = 9$ mmHg at rest in *Octopus*, and using a figure for T_V of 10 mmHg, concluded that arm tissues (muscle and neuropil) would quickly become hypoxic when active.

Sepia. Using our values for R (table 3-7), a diffusion constant k for O_2 through tissues of 0.133×10^{-4} ($\text{cm}^2 \text{ atm}^{-1} \text{ min}^{-1}$ at 15°C , Krogh 1919a), and body O_2 uptake at rest of 1.27×10^{-3} $\text{ml g}^{-1} \text{ min}^{-1}$ (Johansen *et al.* 1982a), we have calculated the $T_0 - T_R$ (in mmHg) in the different tissues at rest (table 10). In all

TABLE 10. CALCULATION OF THE DIFFERENCE IN O_2 TENSION BETWEEN MICROVESSELS AND TISSUE ($T_0 - T_R$) ACCORDING TO THE KROGH-ERLANG EQUATION UNDER DIFFERENT CONDITIONS

tissue	condition	O_2 consumption $\text{ml g}^{-1} \text{ min}^{-1}$ ($\times 10^3$)	$R/\mu\text{m}$	$T_0 - T_R$ mmHg	T_V mmHg
<i>Sepia</i> VL OL VM TM	rest	1.27	28	0.45	18
			20	0.23	
			32	0.77	
			61	3.90	
VL } OL }	rest	10.8*	28	3.82	
			20	1.99	
VL } OL }	50 % microvessel recruitment	10.8*	39	9.18	
			28	4.85	
VL } OL }	increased neural activity (2 times rise in O_2 consumption)	21.6*	28	7.64	
			20	3.98	
VM } TM }	exercise (3 times rise in O_2 consumption)	3.81	32	2.31	
			61	11.70	

* Brain O_2 consumption assumed $8.5 \times$ whole body consumption. Microvessel radius, r : VL 3.25 μm , OL 2.48 μm , VM 2.4 μm , TM 2.05 μm .

cases $T_0 - T_R$ is less than the 18 mmHg T_V measured in *Sepia* (Johansen *et al.* 1982b, figure 3), so that the tissues are adequately supplied with oxygen. If only half the brain vessels are recruited, $T_0 - T_R$ would approximately double, still being within the safety margin provided by the high venous O_2 tension. If neural activity and O_2 consumption increased, probably by no more than twice in normal physiology (Cremer *et al.* 1983), then $T_0 - T_R$ would again double. No figures are available for active *Sepia*, but by comparison with other cephalopods, it is unlikely that O_2 consumption will go up by more than three times in exercise (the figure for squid, O'Dor (1982)), most of the extra oxygen consumption being by muscle. In this case, muscle $T_0 - T_R$ will treble. It is clear than even without a change in blood flow, sufficient oxygen should still reach brain and valve muscle under all

these conditions. In tentacle muscle, a trebling of $T_0 - T_R$ from 3.9 to 11.7 mmHg, if coupled with a drop in T_V in exercise, is likely to lead to muscle hypoxia.

There are some obvious drawbacks to this kind of analysis. Because the blood oxygen tension falls as the blood passes along the microvessel, the distance into the tissue provided with a particular O_2 tension will also fall, so that the analysis should deal with a cone rather than a cylinder of tissue. The analysis does not take into account the real geometrical complexity of vascular networks and flow in the tissues, including counterflow that has been demonstrated in vertebrate brain (Ivanov *et al.* 1979). Our assumptions about the O_2 consumption of muscle may be underestimates, although this is unlikely to be the case for brain. Variables such as the oxygen carrying kinetics of blood and variations in flow are not considered. All of these reservations make it unprofitable to extend the quantitative argument further. However, the Krogh formulation has remained a popular model for comparisons between tissues and species, because no simple alternative models are available. We conclude that when the *Sepia* data are analysed according to the Krogh model, it seems unlikely that the brain should become hypoxic. In muscle, the valve muscle probably receives adequate oxygen even in exercise, while the tentacle muscles might become hypoxic under these conditions.

Correlation with cephalopod biochemistry

The conclusions of our morphometric study correlate well with the known biochemistry of cephalopod tissues. Cephalopod brain has an essentially oxidative metabolism using glucose as substrate (brain hexokinase activity being 15–48 times that of muscle (Ballantyne *et al.* 1981; Storey & Storey 1983), while muscle is either specialized for aerobic, maintained activity (well vascularized, plentiful mitochondria, oxidative enzymes) or anaerobic burst activity (less vascular, fewer mitochondria, glycolytic enzymes) using glycogen and amino acids as substrates (Mommsen *et al.* 1981; Bone *et al.* 1981; Hochachka *et al.* 1983; Storey & Storey 1983). Cephalopods use arginine phosphate rather than creatine phosphate as tissue phosphagen, and octopine dehydrogenase replaces lactate dehydrogenase as the final step of anaerobic glycolysis, producing octopine instead of lactate.

A useful measure of the anaerobic–aerobic capacities of cephalopod tissues is the ratio of the activities of two enzymes, octopine dehydrogenase (ODH) and α -glycerophosphate dehydrogenase (α -GPDH). ODH catalyses the (anaerobic) conjugation of arginine and pyruvate to yield octopine, and α -GPDH reflects the activity of the glycerophosphate cycle which supports aerobic metabolism (Storey & Storey 1983). High ODH/ α -GPDH ratios indicate anaerobic metabolism, low ratios indicate aerobic metabolism.

In representative cephalopods (mainly teuthoids, for which detailed information is available), the ODH/ α -GPDH ratios cover an approximately tenfold range (30–40 in tentacle, arm, and anaerobic mantle muscle, compared with 3 in brain), with aerobic muscles such as fin occupying an intermediate position (7–11) (Baldwin 1982; Storey & Storey 1983). There is thus good correspondence between the cephalopod enzyme ratios, and the reciprocal of the vascularity in *Sepia* (whether measured as Q_A , S_V , or V_V), which also shows an approximately tenfold difference between least and most vascular tissues. This confirms the close correlation between tissue vascularity and oxidative potential in cephalopods.

Comparison of diffusion distances in cephalopods

The values for R of 28 μm (VL) and 20 μm (OL) overall (table 7), and as low as 14–16 μm in OL neuropil (table 8) are in good agreement with the estimates given by J. Z. Young for *Octopus* brain (15–25 μm or more), demonstrating that although the microvessel supply of cephalopod brain has been described as ‘not very rich’ (Young 1971, p. 541), it is nevertheless similar to that of mammalian brain. Our figure for R in *Sepia* tentacle muscle of 61 μm is very close to the 60 μm calculated from Browning’s figure (1982) of $Q_A = 45 \text{ mm}^{-2}$ in *Octopus* arm, indicating that both tissues are specialized for function under relatively anaerobic conditions. The *Octopus* figures suggest that arm neural tissue (axial) is not more vascular than arm muscle (Q_A 45 cf. 44 mm^{-2}), perhaps surprising in view of the known differences in neural and muscle metabolism (Storey & Storey 1983). However, it is not clear whether Browning’s (1982) ‘neuropil’ samples came from axonal or synaptic areas. The low vascularity would suggest regions of axonal tracts rather than synaptic neuropil.

Our values for R in tentacle muscle are also close to the estimated *ca.* 80 μm diffusion distance in the more anaerobic portions of *Alloteuthis* (squid) mantle muscle (Bone *et al.* 1981), while the value of R in valve muscle of 32 μm corresponds well with the 20–30 μm diffusion distance estimated for the more aerobic portions of *Alloteuthis* mantle muscle.

This survey of cephalopod diffusion distances confirms that comparisons can be made between tissues of different species, and distances are similar in tissues of comparable metabolism. While vascularity is undoubtedly low in some tissues specialized for anaerobic function, this is certainly not true for all cephalopod tissues, and in those designed for maximal aerobic performance such as brain, vascular density may be as much as ten times that of anaerobic tissues.

Comparison with the rat

Brain. Values for Q_A , J_V , S_V , \bar{d} , d_m and R in *Sepia* brain are remarkably close to those reported for the rat. The similarities in vascularity of *Sepia* and rat brain are perhaps surprising because the rat has a metabolic rate approximately fourteen times higher; O_2 uptake in rat at rest is 1 $\text{ml g}^{-1} \text{h}^{-1}$ (Arieli & Ar 1981) compared with *Sepia* 0.072 $\text{ml g}^{-1} \text{h}^{-1}$ (measured at 17 °C, Johansen *et al.* (1982a)). Because the body temperatures for the two species differ by 20 °C (*Sepia* 17 °C, rat 37 °C), the rat metabolic rate would be expected to be at least nine times higher simply because of temperature (Q_{10} for metabolic processes *ca.* 3). However, the O_2 carrying capacity of *Sepia* blood is lower (3.4 vol. % (Johansen *et al.* 1982b) compared with rat: 23 vol. % (Gahlenbeck *et al.* 1968)), as is systolic blood pressure. The net result is that the blood is more desaturated as it flows through the tissues, making the gradient of p_{O_2} from microvessel to tissue relatively flat. The high vascularity can be seen as a mechanism to compensate for the deficiencies of the oxygen carrying system, in order to maintain cerebral oxygen supply.

The values for S_V have been used to calculate the permeability (P) of the blood–brain interface from the PS for two non-electrolytes, EDTA and polyethylene glycol (PEG, 4 kDa molecular mass) (Abbott *et al.* 1985b), and show that the *Sepia* blood–brain barrier is as tight as in the rat ($P_{\text{EDTA}} = 3-4 \times 10^{-8} \text{ cm s}^{-1}$,

$P_{PEG} = 1-3 \times 10^{-8}$ cm s⁻¹). The possible effect of microvessel recruitment is unknown (see above), but because this is unlikely to involve more than a doubling of the perfused surface area (Weiss *et al.* 1982; Abbott 1987), it does not greatly affect the conclusion.

Microvascular V_V in *Sepia* appears to be slightly higher than in the rat, which may reflect inclusion of a greater number of larger diameter microvessels (e.g. 14.5% of microvessels in the vertical lobe are in the range 9–20 µm diameter, figure 4). The total vascular V_V is also higher than in the rat, probably because major arterial and venous vessels run in the core of the tissue rather than on the surface.

Muscle. The vascularity of the two *Sepia* muscles used is equivalent to the lower end of the range in rat skeletal muscle, where considerable variation in vascularity has been reported, from fast glycolytic (white) muscle with low vascularity, to slow oxidative (red) muscle with high vascularity (table 7). The estimated S_V values have been used to show that muscle vessels in *Sepia* are much more permeable to extracellular tracers than brain vessels (Abbott *et al.* 1985b).

CONCLUSION

This study represents one of the most comprehensive analyses of tissue vascularity so far attempted in any cold-blooded animal or invertebrate, and should form a useful basis for future physiological and biochemical comparisons with other species. We have shown that cephalopod brain is as densely vascularized as mammalian brain. The vascularity of certain rhythmically active aerobic muscles may approach that of brain, while muscles used exclusively for burst activity have a notably lower vascularity. Calculations using Krogh's formulation show that brain and aerobic valve muscle should receive adequate oxygen even during exercise, while the more anaerobic tentacle muscle may become hypoxic in extreme conditions.

The present estimates of exchange surface area, S_V , have been used to calculate the permeability P of the *Sepia* blood–brain barrier, and it has been shown that in optic lobe, the barrier is as tight as in rat cerebral cortex. It is possible that the blood–brain barrier needs to be tightest in synaptic regions processing complex patterned information (as in vision), because of the need for effective homeostasis around integrating synapses. Effective isolation of the synaptic environment is particularly important in view of the short diffusion distances between blood and synapses demonstrated here.

It is a pleasure to thank Pia Hagman for technical assistance, Bob Roberts for photography, the Director of the Marine Biological Association Laboratory, Plymouth for facilities, and the Wellcome Trust, Nuffield Foundation, and Danish Natural Science Research Council for financial support.

REFERENCES

- Abbott, N. J. 1987 Effect of hypoxia on vascular volume estimates in *Sepia* tissues; evidence for recruitment. (In preparation.)
- Abbott, N. J. & Bundgaard, M. 1985 Vascularity and microvessel surface area density in brain and muscle of the cephalopod *Sepia officinalis*. *J. Physiol., Lond.* **365**, 98P.
- Abbott, N. J., Bundgaard, M. & Cserr, H. F. 1981 Fine-structural evidence for a glial blood-brain barrier to protein in the cuttlefish, *Sepia officinalis*. *J. Physiol., Lond.* **316**, 52P-53P.
- Abbott, N. J., Bundgaard, M. & Cserr, H. F. 1982 Experimental study of the blood-brain barrier in the cuttlefish, *Sepia officinalis* L. *J. Physiol., Lond.* **326**, 43-44P.
- Abbott, N. J., Bundgaard, M. & Cserr, H. F. 1985a Brain vascular volume, electrolytes and blood-brain interface in the cuttlefish, *Sepia officinalis*. *J. Physiol., Lond.* **368**, 197-212.
- Abbott, N. J., Bundgaard, M. & Cserr, H. F. 1985b Tightness of the blood-brain barrier and evidence for interstitial fluid flow in brain of the cuttlefish, *Sepia officinalis*. *J. Physiol., Lond.* **368**, 213-226.
- Arieli, R. & Ar, A. 1981 Blood capillary density in heart and skeletal muscles of the fossorial mole rat. *Physiol. Zool.* **54**, 22-27.
- Bailey, N. T. J. 1983 *Statistical methods in biology*. 2nd edn. London: Hodder & Stoughton.
- Baldwin, J. 1982 Correlations between enzyme profiles in cephalopod muscle and swimming behaviour. *Pacific Sci.* **36**, 349-356.
- Ballantyne, J. S., Hochachka, P. W. & Mommsen, T. P. 1981 The metabolism of the migratory squid *Loligo opalescens*: enzymes of tissues and heart mitochondria. *Mar. Biol. Lett.* **2**, 75-86.
- Bär, T. 1978 Morphometric evaluation of capillaries in different laminae of rat cerebral cortex by automatic image analysis. Changes during development and aging. In *Advances in Neurology*, vol. 20, pp. 1-9. New York: Plenum Press.
- Barber, V. C. & Graziadei, P. 1967 The fine structure of cephalopod blood vessels. II. The vessels of the nervous system. *Z. Zellforsch. mikrosk. Anat.* **77**, 147-161.
- Bone, Q., Pulford, A. & Chubb, A. D. 1981 Squid mantle muscle. *J. mar. biol. Assn. U.K.* **61**, 327-342.
- Bourne, G. B. 1982 Blood pressure in the squid, *Loligo pealei*. *Comp. Biochem. Physiol.* **72A**, 23-27.
- Browning, J. 1982 The density and dimensions of exchange vessels in *Octopus pallidus*. *J. Zool.* **196**, 569-579.
- Bundgaard, M. & Abbott, N. J. 1987 The blood-brain interface of the cephalopod *Sepia officinalis*. I. Fine structure. (In preparation.)
- Bundgaard, M. & Frøkjaer-Jensen, J. 1982 Functional aspects of the ultrastructure of terminal blood vessels: a quantitative study on consecutive segments of the frog mesenteric microvasculature. *Microvascular Res.* **23**, 1-30.
- Cajal, S. R. y 1929 Signification probable de la morphologie des neurones des invertébrés. *Trab. Lab. Invest. biol. Univ. Madrid* **26**, 131-153.
- Conway, R. S. & Weiss, H. R. 1980 Effect of papaverine on regional cerebral blood flow and small vessel blood content. *Eur. J. Pharmacol.* **68**, 17-24.
- Cremer, J. E., Cunningham, V. J. & Seville, M. P. 1983 Relationship between extraction and metabolism of glucose, blood flow, and tissue blood volume in regions of rat brain. *J. cerebral Blood Flow & Metab.* **3**, 291-302.
- Dunning, H. S. & Wolff, H. G. 1937 The relative vascularity of various parts of the central and peripheral nervous system of the cat and its relation to function. *J. comp. Neurol.* **67**, 433-450.
- Gahlenbeck, H., Rathschlag-Schaefer, A. M. & Bartels, H. 1968 Triiodothyronine induced changes of oxygen affinity of blood. *Resp. Physiol.* **6**, 16-22.
- Ghiretti-Magaldi, A., Ghiretti, F. & Salvato, B. 1977 The evolution of haemocyanin. *Symp. zool. Soc. Lond.* **38**, 513-523.
- Graham, R. C. & Karnovsky, M. J. 1966 The early stages of absorption of injected horseradish peroxidase in the proximal tubules of mouse kidney; ultrastructural cytochemistry by a new technique. *J. Histochem. Cytochem.* **14**, 291-302.

- Grimpe, G. 1913 Das Blutgefäßsystem der dibranchiaten Cephalopoden. I. Octopoda. *Z. wiss. Zool.* **104**, 531–621.
- Haynes, J. D. 1964 Estimation of blood vessel surface area and length in tissue. *Nature, Lond.* **201**, 425–426.
- Hochachka, P. W., Fields, J. H. A. & Mommsen, T. P. 1983 Metabolic and enzyme regulation during rest-to-work transition: a mammal versus mollusc comparison. In *The Mollusca* (ed. K. M. Wilbur), vol. 1, pp. 55–89. New York & London: Academic Press.
- Hoppeler, H., Mathieu, O., Weibel, E. R., Krauer, R., Lindstedt, S. L. & Taylor, C. R. 1981 Design of the mammalian respiratory system. VIII. Capillaries in skeletal muscles. *Resp. Physiol.* **44**, 129–150.
- Isgrove, A. 1909 *Eledone*. Liverpool Marine Biological Committee Memoirs, no. 18. Liverpool: University Press.
- Ivanov, K. P., Kislayakov, Y. Y. & Samilov, M. O. 1979 Microcirculation and transport of oxygen to neurones of the brain. *Microvascular Res.* **18**, 434–441.
- Johansen, K., Brix, O., Kornerup, S. & Lykkeboe, G. 1982a Factors affecting O_2 -uptake in the cuttlefish. *J. mar. biol. Assn. U.K.* **62**, 187–191.
- Johansen, K., Brix, O. & Lykkeboe, G. 1982b Blood gas transport in the cephalopod, *Sepia officinalis*. *J. exp. Biol.* **99**, 331–338.
- Krogh, A. 1919a The number and distribution of capillaries in muscles with calculations of the oxygen pressure head necessary for supplying the tissue. *J. Physiol., Lond.* **52**, 409–415.
- Krogh, A. 1919b The supply of oxygen to the tissues and the regulation of the capillary circulation. *J. Physiol., Lond.* **52**, 457–474.
- Levin, V. A., Landahl, H. & Freeman-Dove, M. A. 1976 The application of brain capillary permeability coefficients and the selection of agents which cross the blood–brain barrier. *J. Pharmacokinet. Biopharm.* **4**, 499–519.
- Michel, M. E., Shinowara, N. L., Odman, S. & Rapoport, S. I. 1984 Morphology of endoneurial blood vessels of frog sciatic nerve during vascular perfusion. *Microvascular Res.* **28**, 220–232.
- Mommsen, T. P., Ballantyne, J., MacDonald, D., Gosline, J. & Hochachka, P. W. 1981 Analogues of red and white muscle in squid mantle. *Proc. natn. Acad. Sci. U.S.A.* **78**, 3274–3278.
- O'Dor, R. K. 1982 Respiratory metabolism and swimming performance of the squid *Loligo opalescens*. *Can. J. Fish. aquatic Sci.* **39**, 580–587.
- Packard, A. 1972 Cephalopods and fish: the limits of convergence. *Biol. Rev.* **47**, 241–307.
- Renkin, E. M. 1968 Transcapillary exchange in relation to capillary circulation. *J. gen. Physiol.* **52**, 96s–108s.
- Storey, K. B. & Storey, J. M. 1983 Carbohydrate metabolism in cephalopod molluscs. In *The Mollusca* (ed. K. M. Wilbur), vol. 1, pp. 91–136. New York & London: Academic Press.
- Tompsett, D. H. 1939 *Sepia*. Liverpool Marine Biological Committee Memoirs, no. 32. Liverpool: University Press.
- Weibel, E. R. 1979 *Stereological methods*, vol. 1 (*Practical methods for biological morphometry*). London: Academic Press.
- Weibel, E. R. & Knight, B. W. 1964 A morphometric study on the thickness of the pulmonary air–blood barrier. *J. Cell Biol.* **21**, 367–384.
- Weiss, H. R., Buchweitz, E., Murtha, T. J. & Auletta, M. 1982 Quantitative regional determination of morphometric indices of the total and perfused capillary network in the rat brain. *Circulation Res.* **51**, 494–503.
- Wells, M. J. 1979 The heartbeat of *Octopus vulgaris*. *J. exp. Biol.* **78**, 87–104.
- Wells, M. J. 1983 Circulation in Cephalopods. In *The Mollusca* (ed. E. M. Wilbur), vol. 5, pp. 239–290. New York & London: Academic Press.
- Williams, L. W. 1909 *The anatomy of the common squid Loligo pealei* Lesnew. vol. 55, pp. 1–92. Leiden: E. J. Brill.
- Young, J. Z. 1971 *The anatomy of the nervous system of Octopus vulgaris*. Oxford: Clarendon Press.